DALTON

# Tuning of the electrochemical recognition of substrates as a function of the proton concentration in solution using pH-responsive redox-active receptor molecules

**María José L. Tendero,[a] Angel Benito,[a] Ramón Martínez-Máñez,*[,a] Juan Soto,[a] Jordi Payà,[b] Andrew J. Edwards[c] and Paul R. Raithby[c]**

[a] *Departamento de Química, Universidad Politécnica de Valencia, Camino de Vera s/n, 46071 Valencia, Spain*
[b] *Departamento de Ingeniería de la Construcción, Universidad Politécnica de Valencia, Camino de Vera s/n, 46071 Valencia, Spain*
[c] *Cambridge Centre for Chemical Crystallography, University Chemical Laboratory, University of Cambridge, Lensfield Road, Cambridge CB2 1EW, UK*

Reaction of ferrocene-1,1′-dicarbaldehyde and ethane-1,2-diamine yielded the Schiff-base derivative 2,5,19,22-tetraaza[6.6](1,1′)ferrocenophane-1,5-diene, **1** the molecular structure of which has been determined by single-crystal X-ray analysis. Hydrogenation of **1** with $LiAlH_4$ resulted in the corresponding amine 2,5,19,22-tetraaza-[6.6](1,1′)ferrocenophane **2** which was characterised crystallographically. The protonation behaviour of **2** (denoted as L) and its complex formation with copper(II), nickel(II) and zinc(II) has been studied by potentiometric titrations in tetrahydrofuran–water (70:30 v/v) (0.1 mol $dm^{-3}$ $NBu_4ClO_4$, 25 °C). The complexes $[M(HL)]^{3+}$, $[ML]^{2+}$, $[M(OH)]^{+}$ and $[ML(OH)_2]$ are formed. An electrochemical study of compound **2** has also been performed under the same conditions at which the potentiometry was carried out and the $pK_a$ values for the mixed-valence $Fe^{II}Fe^{III}$ and oxidised $Fe^{III}Fe^{III}$ species determined by fitting the curve of $E_{\frac{1}{2}}$ *versus* pH. From those data the Pourbaix diagram of the redox-active **2** has been calculated. Compound **2** can be considered as a selective electrochemical sensor for copper(II).

There is a considerable interest in the synthesis of compounds bearing electroactive moieties and their use as building blocks in the synthesis of multinuclear systems by self-assembly processes with metal ions. It has been suggested that some of such systems can potentially exhibit intermetallic energy-transfer or electron-transfer processes,[1,2] act as versatile 'electron-reservoir'[1,3] systems or display electrical-conducting or magnetic properties.[4] On the other hand redox-functionalised compounds combine the presence in the same molecule of both co-ordination sites and redox-active moieties. The redox groups in such systems can easily be switched to their oxidised or reduced form giving at least two different states with a different charge as a consequence of adding or withdrawing one or more electrons. Each state is expected to display a different kinetic and thermodynamic behaviour in the binding processes with substrates. Scheme 1 shows the different species that can exist when an electroactive compound (L) and a substrate (S) coexist in solution. Taking into account that both the equilibrium constants ($K_1$ and $K_2$) and the oxidation potentials ($E_1$ and $E_2$) could have a different value, some potential applications have been suggested.

If $K_1 \neq K_2$, the electroactive compound can be a good candidate for driving ions against a chemical concentration gradient by changing its co-ordination ability by oxidation or reduction of the electroactive moieties.[5] On the other hand it has recently been revealed that electroactive compounds can recognise substrates based on the fact that the redox potential $E_1$ is generally different to $E_2$.[6–11] Bearing in mind that different guests can cause a different shift in the redox potential, these kinds of functionalised compounds can be considered as new potential supramolecular electrochemical sensor.

Different redox-active groups have been covalently attached near co-ordination sites but probably the most widely used has been ferrocene, which is known to display reversible single-

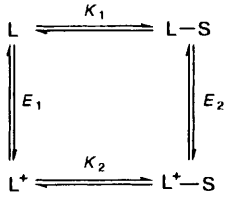


**Scheme 1**

electron processes at modest anodic potentials. Ferrocene has been attached to different binding domains suitable for recognising alkaline- and alkaline-earth-metal ions,[7,8] but relatively less effort has been devoted to the functionalisation of compounds with the ability to display electrochemical recognition processes with transition-metal ions or anions.[9–11] On the other hand, the fact that ferrocene or ferrocene derivatives are usually soluble in organic but not in aqueous solvents due to their non-polar character can sometimes limit the utility of these redox-active compounds.

Polyamines are known to be pH-responsive molecules which can form a large variety of protonated or complexed species as a function of the pH in the medium. The attachment of ferrocenyl units to these systems will produce ferrocene-functionalised polyamines which are simultaneously pH- and redox-responsive molecules and are expected to display a different co-ordination behaviour towards substrates as a function of both the proton concentration and the oxidation state of the ferrocenyl groups. The design of such molecules could lead to the synthesis of new supramolecular sensors or new membrane transport systems where selectivity can be achieved by tuning the pH in the medium. On the other hand, (*i*) ferrocene-functionalised molecules bearing amino groups could be soluble in aqueous media, (*ii*) there are a large number of known polyamines with

different topological arrangements of N-donor groups which could easily be functionalised with ferrocenyl moieties, (*iii*) soluble N-donor compounds could not only co-ordinate transition-metal ions but also act as receptors for anions by both formation of charged species at neutral pH and hydrogen-bond networks.[12]

As a part of our study of redox-active compounds we have developed molecules containing the ferrocenyl group covalently attached to N- and N,O-donor metal-binding domains.[13–15] In this paper we describe the synthesis of the ferrocene-functionalised polyamine 2,5,19,22-tetraaza[6.6](1,1')ferrocenophane, and the study of the effect that co-ordination of $H^+$ and transition-metal ions has on the oxidation potential of the ferrocenyl groups. We will reveal that, using pH-responsive redox-active receptor molecules, the electrochemical recognition of substrates can be modulated as a function of the proton concentration in solution.

## Experimental

### Solvents and reagents

Ethane-1,2-diamine, lithium aluminium hydride, copper(II), nickel(II) and zinc(II) nitrates were reagent quality, used without further purification. Ferrocene-1,1'-dicarbaldehyde was synthesised following literature procedures.[16] Tetrahydrofuran (thf) was freshly distiled from sodium–benzophenone. From this solvent, the thf–water (70:30 v/v) mixture was easily prepared and used as solvent in the potentiometric and electrochemical studies. Carbonate-free potassium hydroxide and hydrochloric acid solutions were used in the potentiometric and electrochemical experiments. Tetrabutylammonium perchlorate (0.1 mol $dm^{-3}$) was used as supporting electrolyte in this solvent mixture.

### Syntheses

**2,5,19,22-Tetraaza[6.6](1,1')ferrocenophane-1,5-diene 1.** A mixture of ferrocene-1,1'-dicarbaldehyde (1 g, 4 mmol) and ethane-1,2-diamine (0.3 $cm^3$, 4 mmol) was refluxed for 2 h in benzene (60 $cm^3$). The resulting orange solution was evaporated to dryness, dissolved in dichloromethane and the compound obtained as an orange solid by addition of hexane (810 mg, 76%) (Found: C, 63.45; H, 5.15; N, 10.50. $C_{28}H_{28}Fe_2N_4$ requires C, 63.20; H, 5.25; N, 10.55%). Infrared spectrum (KBr disc): 1642s, 1467w, 1446w, 1377w, 1283w, 1243m, 1111w, 1001m, 930w, 821m, 678w and 521m $cm^{-1}$. NMR ($CDCl_3$): $^1H$, δ 3.79 (8 H, s, $CH_2$), 4.35 (8 H, t, $C_5H_4$), 4.64 (8 H, t, $C_5H_4$) and 8.21 (4 H, s, CH); $^{13}C$-{$^1H$}, δ 62.12 ($CH_2$), 67.94 ($C_5H_4$), 68.51 ($C_5H_4$), 80.45 ($C_5H_4$, $C_{ipso}$) and 162.23 (CH).

**2,5,19,22-Tetraaza[6.6](1,1')ferrocenophane 2.** Lithium aluminium hydride (304 mg, 8 mmol) was added to a tetrahydrofuran solution (50 $cm^3$) of compound **1** (1064 mg, 2 mmol) under an argon atmosphere. The resulting mixture was refluxed for 1 h, and then small amounts of methanol and water added. The suspension was filtered and the resulting pale yellow solution rotavaporated to dryness and basic water (pH 9, 20 $cm^3$) added. Addition of dichloromethane (3 × 20 $cm^3$) produced yellow organic phases. The dichloromethane solution was then treated with anhydrous magnesium sulfate, filtered and evaporated to dryness. The compound was crystallised from dichloromethane–hexane solutions to yield a yellow powder (850 mg, 79%) (Found: C, 62.35; H, 6.70; N, 10.20. $C_{28}H_{36}Fe_2N_4$ requires C, 62.20; H, 6.65; N, 10.35%). Infrared spectrum (KBr disc): 3072w, 2942w, 2815w, 1474w, 1436s, 1255m, 1095s, 1034s, 870w, 808m, 715s and 495w $cm^{-1}$. NMR ($CDCl_3$): $^1H$, δ 2.02 (4 H, br, NH), 2.92 (8 H, s, $CH_2$), 3.48 (8 H, s, $CH_2$), 4.10 (8 H, t, $C_5H_4$) and 4.23 (8 H, t, $C_5H_4$); $^{13}C$-{$^1H$}, δ 48.41 ($CH_2$), 49.04 ($CH_2$), 67.52 ($C_5H_4$), 68.21 ($C_5H_4$) and 88.36 ($C_5H_4$, $C_{ipso}$).

### Physical measurements

The NMR spectra were measured on a Bruker AC-200 FT spectrometer operating at 300 K. Chemical shifts for $^1H$ and $^{13}C$-{$^1H$} are referenced to $SiMe_4$ and $CDCl_3$. Infrared spectra were taken on a Perkin-Elmer 1750 spectrophotometer as KBr pellets. Cyclic voltammograms were obtained with a Tacusel IMT-1 programmable function generator, connected to a Tacusel PJT 120-1 potentiostat. The working electrode was platinum with a saturated calomel reference electrode (SCE) separated from the test solution by a salt bridge containing the solvent/supporting electrolyte. The auxiliary electrode was platinum wire. Potentiometric titrations were carried out in thf–water (70:30 v/v) under nitrogen using a reaction vessel water-thermostatted at 25.0 ± 0.1 °C. The titrant was added by a Crison 2031 microburette. The potentiometric measurements were made using a Crison 2002 pH-meter and a combined glass electrode. The titration system was automatically controlled by a personal computer using a program which monitors the electromotive force values and the volume of titrant added. The electrode was dipped in thf–water (70:30 v/v) for 0.5 h before use. It was calibrated as a hydrogen-concentration probe by titration of well known amounts of HCl with $CO_2$-free KOH solution and determining the equivalence point by Gran's method[17] which gives the standard potential $E'°$ and the ionic product of water ($K'_w = [H^+][OH^-]$). The logarithm of $K'_w$ for the solvent used was found to be −16.2 ± 0.2 (25 °C, 0.1 mol $dm^{-3}$ $NBu_4ClO_4$). The concentrations of the copper(II), nickel(II) and zinc(II) solutions were determined gravimetrically using standard methods. The computer program SUPERQUAD[18] was used to calculate the protonation and stability constants.

### Structure determinations

**Compound 1.** *Crystal data.* $C_{28}H_{28}Fe_2N_4$, $M$ = 532.24, monoclinic, space group $C2/c$, $a$ = 29.652(6), $b$ = 9.939(2), $c$ = 8.116(2) Å, β = 96.70(3)°, $U$ = 2375.5(9) $Å^3$, $Z$ = 4, $D_c$ = 1.488 g $cm^{-3}$, λ(Mo-Kα) = 0.710 69 Å, crystal size 0.21 × 0.19 × 0.14 mm, μ = 12.5 $cm^{-1}$.

*Data collection and refinement.* A well shaped orange crystal was mounted on a Rigaku AFC7 four-circle diffractometer coupled to a molybdenum-target rotating-anode X-ray source. Unit-cell dimensions were determined from the angular settings of 25 reflections. A monoclinic cell was obtained and the space group $C2/c$ was confirmed from the structure determination. A total of 2138 reflections were measured of which 2096 were unique ($R_{int}$ = 0.022) ($5.5 \leqslant 2\theta \leqslant 50.0°$) using the 2θ–ω method. The intensity of three standard reflections monitored every 60 min showed no systematic variation. 1644 Reflections were considered as observed with $F > 4\sigma(F)$. Lorentz and polarisation corrections were applied but not for absorption. The structure was solved by direct methods (SHELXTL PLUS)[19] and refined by full-matrix least squares on $F^2$ (SHELXL 93).[20] The refinement converged at $R1$ 0.040 [$F > 4\sigma(F)$, for 1644 reflections] and $R2$ 0.109 (all data). Largest peak and hole in the final difference map +0.26, −0.34 e $Å^{-3}$.

**Compound 2.** *Crystal data.* $C_{28}H_{36}Fe_2N_4$, $M$ = 540.31, monoclinic, space group $C2/c$, $a$ = 21.203(4), $b$ = 21.140(4), $c$ = 23.272(5) Å, β = 102.40(3)°, $U$ = 10 188(4) $Å^3$, $Z$ = 16, $D_c$ = 1.409 g $cm^{-3}$, λ(Mo-Kα) = 0.710 69 Å, crystal size 0.35 × 0.22 × 0.18 mm, μ = 11.6 $cm^{-1}$.

*Data collection and refinement.* A pale yellow crystal grown by diffusion of hexane into dichloromethane solutions of compound **2** was used. X-Ray intensities were recorded as for **1**. From the angular setting of 25 reflections, a $C$-centred

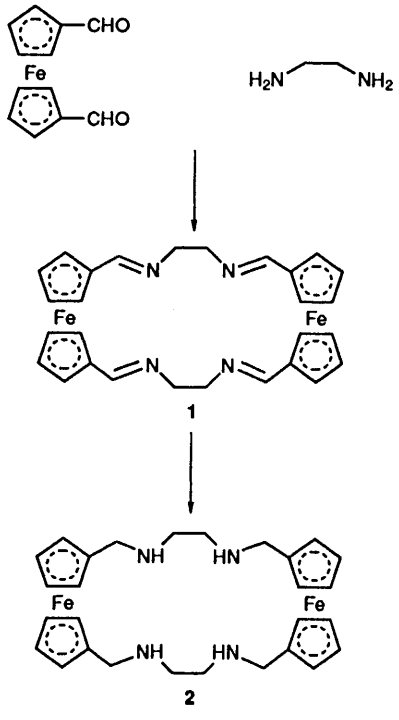


Scheme 2

monoclinic cell was obtained, and the space group $C2/c$ was confirmed from the structure determination. A total of 6848 reflections were measured ($5.2 \leqslant 2\theta \leqslant 45.0°$) using the $2\theta$–$\omega$ technique. Three standard reflections as for **1**. 6634 Reflections were unique ($R_{int} = 0.039$) of which 3371 were observed [$F > 4\sigma(F)$]. Corrections applied and structure solution as for **1** gave $R1$ 0.085 [$F > 4\sigma(F)$, for 3371 reflections] and $R2$ 0.239 (all data). Largest peak and hole in the final difference map $+0.73$, $-0.35$ e Å$^{-3}$.

Complete atomic coordinates, thermal parameters and bond lengths and angles have been deposited at the Cambridge Crystallographic Data Centre. See Instructions for Authors, *J. Chem. Soc., Dalton Trans.*, 1996, Issue 1.

## Results and Discussion

### Synthesis and characterization

Ferrocene-1,1′-dicarbaldehyde reacts with ethane-1,2-diamine (1:1 molar ratio) to produce orange solutions from which the Schiff-base derivative **1** was isolated in a good yield (Scheme 2). It shows a characteristic strong ν(C=N) stretching vibration at 1642 cm$^{-1}$. The $^1$H NMR spectrum exhibits only four signals indicating that the molecule is highly symmetric in solution. Two of these, at δ 4.35 and 4.64, are pseudo-triplets and are attributed to the two non-equivalent protons in the cyclopentadienyl rings. The signal at δ 3.79 is assigned to the presence of a $CH_2$ group whereas the protons of the imino moiety appear at δ 8.21. The $^{13}$C-{$^1$H} NMR spectrum shows three resonances in the range δ 67.94–80.45 attributed to the cyclopentadienyl rings, the remainder at δ 62.12 and 162.23 are assigned to the $CH_2$ and Schiff-base groups, respectively. The mass spectrum (FAB, $m/z$ 533) and the elemental analysis are in agreement with the proposed formulation.

The reaction of ferrocene-1,1′-dicarbaldehyde with ethane-1,2-diamine to yield the bis(ferrocene)derivative **1** contrasts with the reactivity found with trimethylenediamine.[21] Under the same conditions the monoferrocene derivative 1,1′-(2,6-diazahepta-1,6-diene-1,7-diyl)ferrocene was found as unique product. A similar behaviour has been reported when other polyamines react with ferrocene-1,1′-dicarbaldehyde to produce 1,1′-ferrocene derivatives.[9] The different reactivity between ethane-1,2-diamine and trimethylenediamine seems to be related with the fact that the former is not long enough to produce monoferrocene derivatives without producing considerable strains in the molecule.

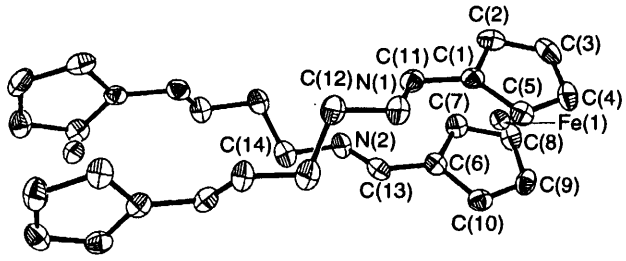


**Fig. 1** Crystal structure of compound **1** showing the atomic numbering scheme

**Table 1** Atomic coordinates ($\times 10^4$) for compound **1**

| Atom | $x$ | $y$ | $z$ |
|---|---|---|---|
| Fe(1) | 1653(1) | 7601(1) | 1446(1) |
| N(1) | 375(1) | 6996(3) | −524(4) |
| N(2) | 777(1) | 8166(3) | 4804(4) |
| C(1) | 1157(1) | 6440(3) | 163(4) |
| C(2) | 1506(1) | 5617(4) | 998(5) |
| C(3) | 1921(1) | 5962(4) | 395(5) |
| C(4) | 1832(1) | 7001(4) | −799(4) |
| C(5) | 1363(1) | 7293(3) | −946(4) |
| C(6) | 1376(1) | 8713(3) | 3210(4) |
| C(7) | 1734(1) | 7880(4) | 3959(4) |
| C(8) | 2136(1) | 8235(4) | 3277(4) |
| C(9) | 2030(1) | 9278(4) | 2111(4) |
| C(10) | 1565(1) | 9570(3) | 2064(4) |
| C(11) | 679(1) | 6409(3) | 435(4) |
| C(12) | −92(1) | 6888(4) | −155(5) |
| C(13) | 904(1) | 8718(3) | 3551(4) |
| C(14) | 297(1) | 8261(4) | 5045(5) |

**Table 2** Selected bond lengths (Å) and angles (°) for compound **1**

| | | | |
|---|---|---|---|
| Fe(1)–C(8) | 2.038(3) | Fe(1)–C(3) | 2.042(4) |
| Fe(1)–C(2) | 2.043(4) | Fe(1)–C(9) | 2.045(3) |
| Fe(1)–C(7) | 2.045(3) | Fe(1)–C(10) | 2.045(3) |
| Fe(1)–C(4) | 2.045(3) | Fe(1)–C(6) | 2.054(3) |
| Fe(1)–C(5) | 2.053(3) | Fe(1)–C(1) | 2.055(3) |
| N(1)–C(11) | 1.262(4) | N(1)–C(12) | 1.454(4) |
| N(2)–C(13) | 1.251(4) | N(2)–C(14) | 1.461(4) |
| C(1)–C(11) | 1.462(5) | C(12)–C(14$^I$) | 1.502(6) |
| C(6)–C(13) | 1.459(5) | | |
| C(14)–N(2)–C(13) | 118.0(3) | C(11)–N(1)–C(12) | 117.8(3) |

Symmetry relation = I $-x, y, -z + \frac{1}{2}$.

X-Ray single-crystal studies were performed on compound **1**. Suitable crystals were obtained by slow diffusion of hexane into a solution of the compound in dichloromethane. Final atomic coordinates for non-hydrogen atoms and selected bond distances and angles are listed in Tables 1 and 2, respectively. A view of the molecule is depicted in Fig. 1. The structure consists of a ring built with two ferrocenyl units bridged by two 2,5-diazahexa-1,5-diene groups which are covalently attached to the cyclopentadienyl rings. Half of the molecule is symmetrically related with the other half in the crystal by an inversion centre located in the centre of the molecule. The cyclopentadienyl rings were found to be planar within experimental error. Atom Fe(1) lies 1.653 Å from both planes C(1)–C(5) and C(6)–C(10). The Fe(1)–C($C_5H_4$) bond lengths range from 2.038(3) to 2.055(3) Å, averaging 2.047(3) Å, and C($C_5H_4$)–C($C_5H_4$) distances are 1.406(6)–1.427(5) Å, averaging 1.419(5) Å. The ferrocenyl unit is in an eclipsed conformation with a twist angle of 2.2°. Some dihedral angles are: C(6)–C(13)–N(2)–C(14) 178.5, C(13)–N(2)–C(14)–C(12$^I$) 122.4, N(2)–C(14)–C(12$^I$)–N(1$^I$) 175.5,

**Table 3** Atomic coordinates ( $\times 10^4$) for compound **2**

| Atom | *x* | *y* | *z* | Atom | *x* | *y* | *z* |
|---|---|---|---|---|---|---|---|
| Fe(1) | 3761(1) | 5783(1) | 1596(1) | Fe(3) | 3422(1) | 476(1) | 1622(1) |
| Fe(2) | 851(1) | 8038(1) | 1591(1) | Fe(4) | 1163(1) | 3373(1) | 1574(1) |
| N(1) | 1644(4) | 5807(5) | 1064(5) | N(5) | 1750(7) | 78(7) | 1103(7) |
| N(2) | 306(8) | 6533(9) | 1072(8) | N(6) | 1077(5) | 1363(5) | 1077(5) |
| N(3) | 2755(5) | 8022(5) | 1123(5) | N(7) | 2675(5) | 3751(5) | 1146(5) |
| N(4) | 4033(5) | 7399(5) | 1162(5) | N(8) | 3285(5) | 2487(5) | 1131(5) |
| C(1) | 4196(6) | 6288(7) | 1052(7) | C(31) | 3401(6) | 1431(5) | 1532(6) |
| C(2) | 4646(5) | 6155(7) | 1573(6) | C(32) | 4006(6) | 1239(6) | 1862(6) |
| C(3) | 4687(7) | 5477(8) | 1645(8) | C(33) | 3888(7) | 910(6) | 2373(6) |
| C(4) | 4265(8) | 5220(8) | 1138(9) | C(34) | 3208(8) | 907(6) | 2343(6) |
| C(5) | 3956(7) | 5709(9) | 780(7) | C(35) | 2919(6) | 1221(6) | 1824(6) |
| C(6) | 3034(5) | 6324(6) | 1781(6) | C(36) | 3349(12) | 98(7) | 808(7) |
| C(7) | 3474(6) | 6141(7) | 2313(6) | C(37) | 3906(9) | −118(8) | 1178(9) |
| C(8) | 3484(6) | 5481(7) | 2336(6) | C(38) | 3764(7) | −423(7) | 1653(8) |
| C(9) | 3064(5) | 5254(6) | 1826(6) | C(39) | 3074(7) | −421(6) | 1585(6) |
| C(10) | 2779(5) | 5757(6) | 1474(5) | C(40) | 2827(8) | −84(7) | 1049(7) |
| C(11) | 2285(6) | 5747(7) | 921(6) | C(41) | 2105(11) | 96(11) | 733(9) |
| C(12) | 1128(7) | 5735(7) | 540(6) | C(42) | 1041(7) | 273(7) | 743(8) |
| C(13) | 489(6) | 5869(8) | 706(7) | C(43) | 882(7) | 951(7) | 563(6) |
| C(14) | 353(13) | 6849(14) | 669(9) | C(44) | 975(7) | 2030(6) | 919(6) |
| C(15) | 138(6) | 7533(8) | 1049(8) | C(45) | 1117(6) | 2427(6) | 1471(5) |
| C(16) | −52(6) | 7704(7) | 1570(7) | C(46) | 676(6) | 2631(6) | 1812(6) |
| C(17) | −42(6) | 8378(8) | 1620(8) | C(47) | 1039(7) | 2934(6) | 2319(6) |
| C(18) | 158(7) | 8610(10) | 1131(9) | C(48) | 1696(6) | 2933(6) | 2298(6) |
| C(19) | 279(6) | 8123(11) | 781(7) | C(49) | 1753(6) | 2609(5) | 1779(6) |
| C(20) | 1660(5) | 7486(6) | 1804(6) | C(50) | 891(8) | 3758(7) | 765(6) |
| C(21) | 1460(6) | 7674(7) | 2310(6) | C(51) | 493(7) | 3980(7) | 1134(8) |
| C(22) | 1465(6) | 8328(7) | 2339(6) | C(52) | 879(7) | 4296(6) | 1613(8) |
| C(23) | 1650(6) | 8561(6) | 1836(6) | C(53) | 1521(6) | 4261(6) | 1537(7) |
| C(24) | 1781(5) | 8032(6) | 1503(6) | C(54) | 1534(7) | 3941(6) | 1005(6) |
| C(25) | 2051(6) | 8053(8) | 949(6) | C(55) | 2104(8) | 3756(8) | 718(7) |
| C(26) | 3071(6) | 8102(7) | 626(6) | C(56) | 3215(7) | 3581(6) | 840(7) |
| C(27) | 3787(7) | 8012(7) | 862(7) | C(57) | 3259(7) | 2927(6) | 639(6) |
| C(28) | 3974(8) | 6913(7) | 752(6) | C(58) | 3290(7) | 1815(6) | 974(6) |

**Table 4** Selected bond lengths (Å) and angles (°) for compound **2**

| | | | |
|---|---|---|---|
| Fe(3)–C(40) | 2.12(14) | Fe(3)–C(35) | 2.013(12) |
| Fe(3)–C(31) | 2.029(12) | Fe(3)–C(38) | 2.030(13) |
| Fe(3)–C(39) | 2.030(12) | Fe(3)–C(36) | 2.03(2) |
| Fe(3)–C(33) | 2.033(12) | Fe(3)–C(37) | 2.04(2) |
| Fe(3)–C(32) | 2.038(12) | Fe(3)–C(34) | 2.045(12) |
| Fe(4)–C(45) | 2.015(13) | Fe(4)–C(50) | 2.016(14) |
| Fe(4)–C(46) | 2.020(12) | Fe(4)–C(51) | 2.021(13) |
| Fe(4)–C(53) | 2.032(12) | Fe(4)–C(47) | 2.034(12) |
| Fe(4)–C(49) | 2.037(11) | Fe(4)–C(48) | 2.041(13) |
| Fe(4)–C(52) | 2.049(13) | Fe(4)–C(54) | 2.063(13) |
| C(41)–N(5) | 1.26(2) | N(5)–C(42) | 1.61(2) |
| C(43)–N(6) | 1.46(2) | N(6)–C(44) | 1.46(2) |
| C(55)–N(7) | 1.39(2) | N(7)–C(56) | 1.52(2) |
| C(57)–N(8) | 1.467(14) | N(8)–C(58) | 1.47(2) |
| C(41)–N(5)–C(42) | 105(2) | C(43)–N(6)–C(44) | 111.6(11) |
| C(55)–N(7)–C(56) | 107.1(12) | C(57)–N(8)–C(58) | 114.9(10) |

C(1)–C(11)–N(1)–C(12) 179.2, C(11)–N(1)–C(12)–C($14^I$) 125.9 and N(1)–C(12)–C($14^I$)–N($2^I$) 175.5°. The complex shows a helical conformation with an angle between the planes C(1)–C(5) and C($6^I$)–C($10^I$) of 86.4°.

Compound **1** could potentially act as an N-donor tetradentate ligand. However, we have recently found that Schiff-base moieties bearing a ferrocenyl unit can be unstable in solution due to hydrolysis in the presence of water or metal ions.[13,14] Hence, we have not attempted any co-ordination studies on **1** and decided to reduce the imino groups to secondary amines. Reaction of **1** with $LiAlH_4$ in freshly distilled tetrahydrofuran gave compound **2**. The FAB mass spectrum of this solid shows an ion at *m/z* 541. The $^1H$ NMR spectrum exhibits five signals indicating that the compound is symmetric on the NMR time-scale. Two pseudo-triplets at δ 4.10 and 4.23 are assigned to the α- and β-protons in the ferrocenyl groups, whereas two singlets at δ 2.92 and 3.48 are attributed to the two non-equivalent $CH_2$ groups. An additional broad signal at δ 2.02 is due to the presence of HN moieties. The $^{13}C$-{$^1H$} NMR spectrum shows five signals, three of which are assignable to the α-, β- and *ipso*-carbons from the ferrocenyl groups (δ 67.52, 68.21, 88.36) whereas the other two correspond to the presence of two non-equivalent $CH_2$ groups (δ 48.41, 49.04).

Suitable crystals of compound **2** were obtained from slow diffusion of hexane into dichloromethane solutions of it. Final atomic coordinates for non-hydrogen atoms and selected bond distances and angles are listed in Tables 3 and 4, respectively. The structure shows two ferrocenyl units bridged by two 2,5-diazahexane moieties. Two molecules were found in the asymmetric unit (see Fig. 2). Fig. 2(*c*) shows an alternative view of the two molecules although not in the actual relative orientation in the crystal. Although the two molecules are related by a mirror plane they appear not to be enantiomers because it seems they can be converted into each other by a twist of the cyclopentadienyl rings. The iron–cyclopentadienyl distances range from 1.632 to 1.646 Å, averaging 1.640 Å. The Fe–C($C_5H_4$) distances range from 2.002(13) to 2.063(13) Å [average 2.032(13) Å] and intracyclopentadienyl C–C bond lengths lie in the range 1.37(2)–1.45(2) Å [average 1.41(2) Å]. Some limitations to the accuracy of the experimental data were found. Disorder appears to affect one of the two 2,5-diazahexane groups and some atoms modelled highly anisotropically. This is most apparent for C(14) which gives meaningless bond lengths, for example C(14)–C(15) 1.81(3) Å. However no well defined peaks were found near C(14) and no attempts were made to model the disorder. The geometry of **2** can be adequately described by the torsion angles N(1)–C(12)–C(13)–N(2) 51.8, N(4)–C(27)–C(26)–N(3) 58.3, N(5)–C(42)–C(43)–N(6) 50.8 and N(8)–C(57)–C(56)–N(7) 54.9°.

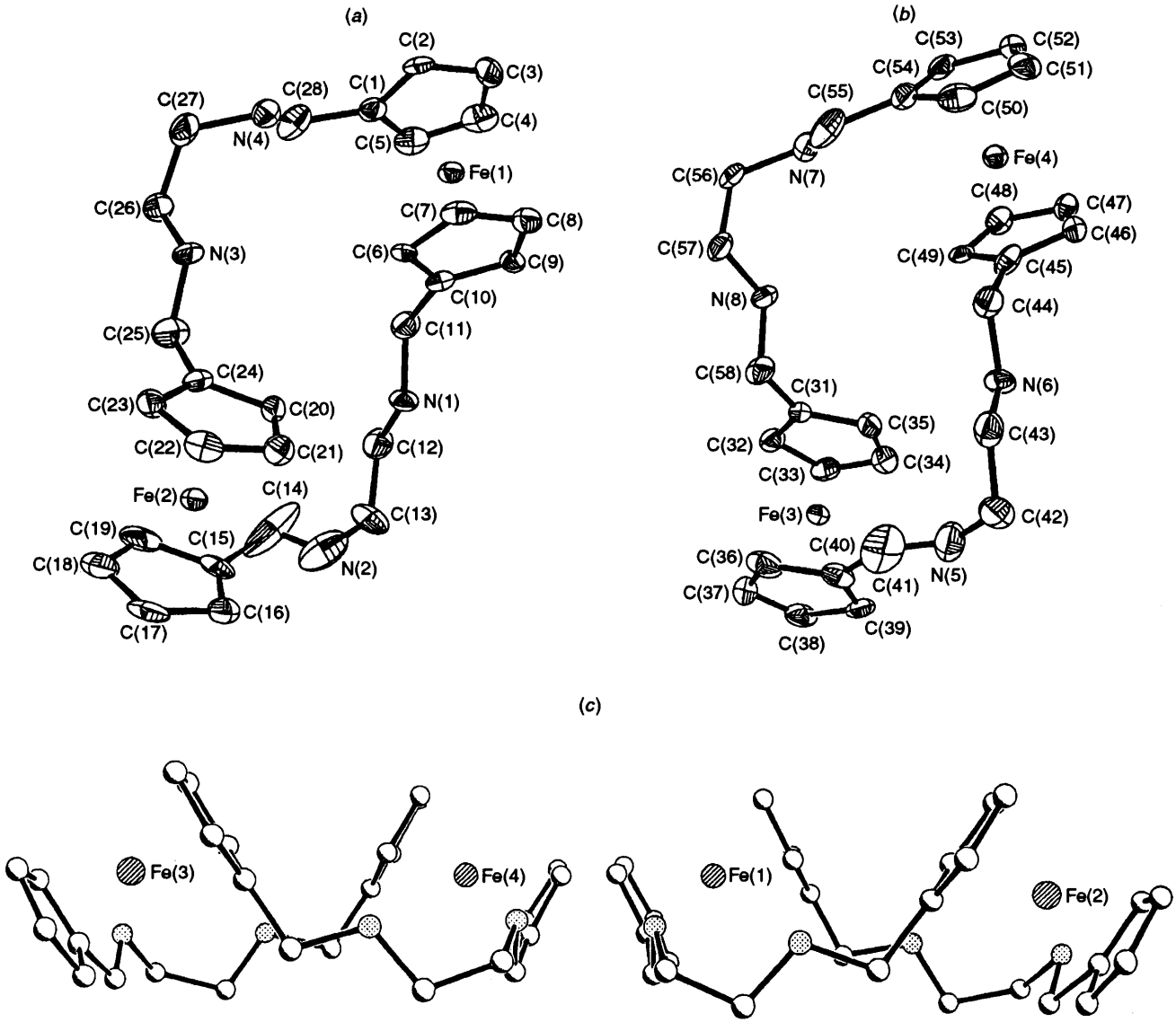


**Fig. 2** Crystal structure of compound **2** showing the two molecules [(*a*) and (*b*)] in the asymmetric unit. An alternative representation of these two molecules is shown in (*c*). The figure does not show the actual relative orientation of the molecules in the crystal

### Potentiometric studies

The protonation of compound **2** was investigated by potentiometric titrations with KOH of previously acidified solutions of **2**. Although **2** is soluble in aqueous acid it precipitates at neutral pH. Therefore thf–water (70:30 v/v) was employed as solvent. Other solvent mixtures as dimethyl sulfoxide–water or dioxane–water could not be used because of the insolubility of **2**. Data processed with the SUPERQUAD[18] program for the **2**–$H^+$ system allowed us to determine the corresponding protonation constants. In Table 5 the basicity constants of **2** together with those of the related molecules 1,4,8,11-tetraazacyclotetradecane (cyclam) and *N*,*N*′-bis(ferrocenylmethyl)ethane-1,2-diamine, (fcmen) are listed.

At pH > 10.5 only the non-protonated species **2** is present. When the pH decreases successive protonation processes are observed. At neutral pH mono- and di-protonated species co-exist. The first two protonation constants for **2** are close to those of the related fcmen.[13] On the other hand **2** behaves as a strong acid when the first two protonation steps are compared with cyclam, but as a strong base when the last two are taken into account.[23]

We have also studied potentiometrically the complex formation of compound **2** (denoted L) with copper(II), nickel(II) and zinc(II). The distribution diagram of the **2**–$H^+$–$Cu^{II}$ equilibria is depicted in Fig. 3, whereas the stability constants are gathered in Table 6. The complex $[CuL]^{2+}$ is predominant over a wide pH range (5.2–10.8). From pH 3 to 6 this complex coexists with $[Cu(HL)]^{3+}$ and unco-ordinated copper(II). At pH > 9 $[CuL]^{2+}$ and the hydroxo species $[CuL(OH)]^+$ coexist. The value of the stability constant of $[CuL]^{2+}$ is seventeen orders of magnitude smaller than that of $[Cu(cyclam)]^{+}$[2] (log $K$ = 27.2),[24] and six orders of magnitude smaller than that of $[Cu(fcmen)_2]^{2+}$ (log $K$ = 16.00)[13] probably due to molecular strains. For copper(II) only experimental data belonging to the range pH 2–10.5 were computed because of the precipitation of a brown solid at pH > 10.5.

**Table 5** Basicity constants (log $K$)[a] for compound **2** (denoted L) in thf–water (70:30 v/v) (25 °C, 0.1 mol $dm^{-3}$ $NBu_4ClO_4$)

| Reaction | **2** | cyclam[b] | fcmen[c] |
|---|---|---|---|
| $L + H^+ \rightleftharpoons HL^+$ | 8.40(1) | 11.585(5) | 9.40(1) |
| $HL^+ + H^+ \rightleftharpoons H_2L^{2+}$ | 6.71(1) | 10.624(4) | 6.40(1) |
| $H_2L^{2+} + H^+ \rightleftharpoons H_3L^{3+}$ | 5.15(1) | 1.61(1) | — |
| $H_3L^{3+} + H^+ \rightleftharpoons H_4L^{4+}$ | 2.45(3) | 2.42(1) | — |

[a] Values in parentheses are the standard deviations in the last significant digit. [b] Data taken from ref. 22 [water, 25 °C, $I$ = 0.5 ($KNO_3$)]. [c] Data taken from ref. 13 [$Me_2SO$–water (80:20 v/v), 25 °C, 0.1 mol $dm^{-3}$ $KClO_4$].

The distribution diagram of the $Ni^{II}$–**2**–$H^+$ system is depicted in Fig. 4. At pH $\geqslant 4$ the complexes $[Ni(HL)]^{3-}$, $[NiL]^{2+}$ and $[NiL(OH)]^+$ coexist over a wide pH range. The stability constant of $[NiL]^{2+}$ is two orders of magnitude smaller than that of the corresponding copper(II) complex (see Table 6). The dihydroxo complex $[NiL(OH)_2]$ exists at pH > 7. Data at pH > 8.5 were not computed due to the precipitation of a yellow-brown solid.

The distribution diagram of the $Zn^{II}$–**2**–$H^+$ system is similar to that of nickel(II) with the coexistence of the species $[Zn(HL)]^{3+}$, $[ZnL]^{2+}$, $[ZnL(OH)]^+$ and $[ZnL(OH)_2]$. Only data in the range pH 2–8.2 were computed because of the precipitation of a yellow solid. For nickel(II) and zinc(II) this solid is probably related to the neutral complexes $[ML(OH)_2]$, however all our attempts to characterise them unequivocally have been unsuccessful.

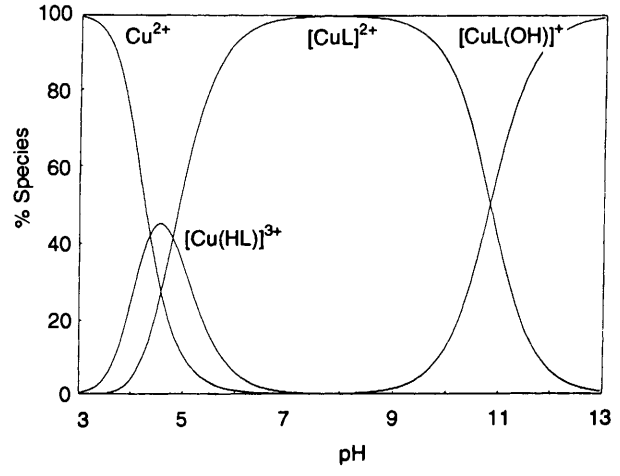


**Fig. 3** Distribution diagram for the **2**–$H^+$–$Cu^{2+}$ system as a function of pH

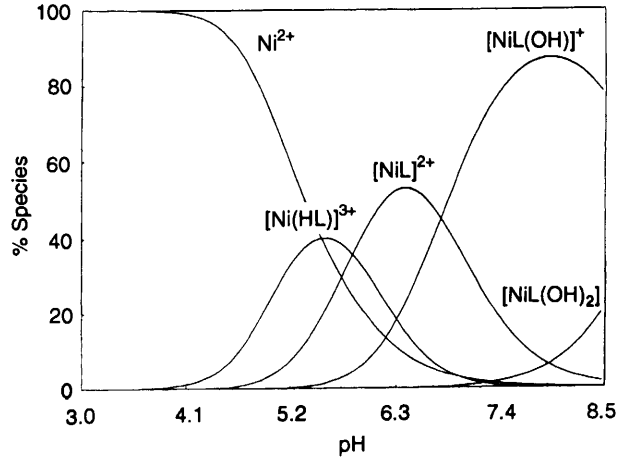


**Fig. 4** Distribution diagram for the **2**–$H^+$–$Ni^{2+}$ system as a function of pH

**Electrochemical study**

Compound **2** is an electroactive species bearing two ferrocenyl groups which are expected to be easily oxidised. That means that each $H_jL^{j+}$ species which exists in solution as a function of the pH may be switched by electrical energy to three different states; the 'reduced' species $Fe^{II}Fe^{II}$ (overall charge $j+$), the mixed-valence species $Fe^{II}Fe^{III}$ $[(j+1)^+]$ and the oxidised species $Fe^{III}Fe^{III}$ $[(j+2)^+]$. This means a total of fifteen different complexes which can exist as a function of both the pH and the potential applied. We have undertaken an electrochemical study of free **2** as a function of pH under the same conditions at which the potentiometric measurements were carried out. Compound **2** was dissolved in acidified thf–water (70:30 v/v) under nitrogen in reaction vessel thermostatted at 25 °C. As in the potentiometric titrations, 0.1 mol $dm^{-3}$ $NBu_4ClO_4$ was used as supporting electrolyte. The pH was measured with a previously calibrated glass electrode. In the reaction vessel a platinum working electrode, a calomel reference electrode and an auxiliary platinum-wire electrode were dipped. When the electrochemical measurements were taken the glass electrode was removed from the solution in order to prevent the potential imposed by the potentiostat from affecting the pH electrode.

We have found that an accurate determination of the half-wave potential ($E_{\frac{1}{2}}$) as a function of the proton concentration in solution can be obtained by using rotating-disc electrode techniques. In all the pH range studied an unique wave was observed. Fig. 5 shows a plot of $E_{\frac{1}{2}}$ *versus* pH for compound **2**. About pH 2 the oxidation potential of the ferrocenyl groups was found to be 611 mV *versus* SCE. From pH 2 to 5 a displacement of $E_{\frac{1}{2}}$ to more cathodic potentials occurs. From pH 5 to 8 the slope of the curve increases coinciding with the formation of the $H_2L^{2+}$ and $HL^+$ species (both $Fe^{II}Fe^{II}$). From pH 8 to 10 the $E_{\frac{1}{2}}$ shifts about 30 mV. At pH > 10 no further change in the oxidation potential was found in agreement with the fact that L is the unique form in solution.

Recently, it has been reported that the redox potentials of the ammonium salts of ferrocene nitrogen containing compounds are shifted by 100–600 mV relative to those of neutral ferrocene.[22] It has also been revealed that there is a relationship between the iron–nitrogen distance and the shift of the redox potentials. We recently found a shift of near 280 mV when acid was added to 2-ferrocenylbenzimidazole using a mixture of

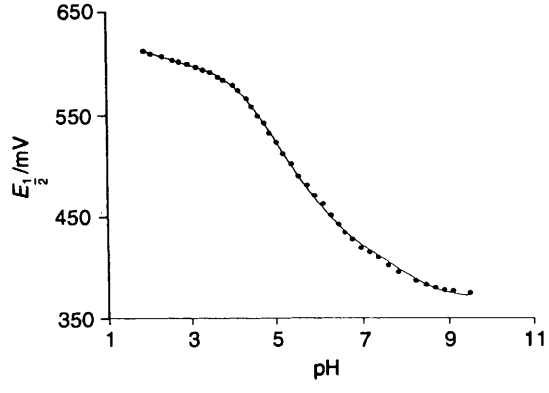


**Fig. 5** Plot of the half-wave potential ($E_{\frac{1}{2}}$) *versus* pH for compound **2** showing the better fit for $n = 1$

**Table 6** Formation constants (log *K*) for complexes of $Cu^{II}$, $Ni^{II}$ and $Zn^{II}$ with compound **2** (denoted L) in thf–water (70:30 v/v) at 25 °C and 0.1 mol $dm^{-3}$ KCl*

| Reaction | $Ni^{II}$ | $Zn^{II}$ | $Cu^{II}$ |
|---|---|---|---|
| $M^{2+} + L + H^+ \rightleftharpoons [M(HL)]^{3+}$ | 12.86(1) | 12.69(1) | 14.71(1) |
| $M^{2+} + L \rightleftharpoons [ML]^{2+}$ | 7.01(1) | 6.63(1) | 9.93(1) |
| $M^{2+} + L + H_2O \rightleftharpoons [ML(OH)]^+ + H^+$ | 0.25(2) | −0.59(2) | −0.86(2) |
| $M^{2+} + L + 2H_2O \rightleftharpoons [ML(OH)_2] + 2H^+$ | −8.79(4) | −8.26(2) | — |

* Values in parentheses are the standard deviations in the last significant digit.

$CH_2Cl_2$–MeOH as solvent.[25] The data obtained for compound **2** reveal that the presence of charged groups produces a large change in redox potential of the ferrocenyl moieties and therefore a similar large shift is expected when **2** co-ordinates to other charged substrates.

The processes occurring at the electrode can be described as in Scheme 3, where $K_n$, $K_n'$ and $K_n''$ are the acid-dissociation constants for the 'reduced', mixed-valence and oxidised species, respectively. If the equilibria proposed in Scheme 3 are correct, equation (1) should fit the curve in Fig. 5,[26,27] where $n$

$$E = E^\circ_{\frac{1}{2}} + \frac{RT}{nF} \ln \frac{a_{red}}{a_{ox}} \quad (1)$$

represents the number of electrons. When $n = 1$, $E^\circ_{\frac{1}{2}}$ is the half-wave potential of the couple $H_4L^{4+}(Fe^{II}Fe^{II})$–$H_4L^{5+}(Fe^{II}Fe^{III})$ at pH 0 and $a_{red}$ and $a_{ox}$ are as in equations (2) and (3)

$$a_{red} = K_1K_2K_3K_4 + K_1K_2K_3[H^+] + K_1K_2[H^+]^2 + K_1[H^+]^3 + [H^+]^4 \quad (2)$$

$$a_{ox} = K_1'K_2'K_3'K_4' + K_1'K_2'K_3'[H^+] + K_1'K_2'[H^+]^2 + K_1'[H^+]^3 + [H^+]^4 \quad (3)$$

respectively. When $n = 2$, $E^\circ_{\frac{1}{2}}$ is the half-wave potential of $H_4L^{4+}(Fe^{II}Fe^{II})$–$H_4L^{6+}(Fe^{III}Fe^{III})$ at pH 0 and $a_{red}$ and $a_{ox}$ are as in equations (2) and (4). A non-linear regression fit of $E_{\frac{1}{2}}$

$$a_{ox} = K_1''K_2''K_3''K_4'' + K_1''K_2''K_3''[H^+] + K_1''K_2''[H^+]^2 + K_1''[H^+]^3 + [H^+]^4 \quad (4)$$

*versus* pH for $n = 1$ and 2 provided the acid-dissociation constants for the mixed-valence species $H_jL^{(j+1)+}$ ($Fe^{II}Fe^{III}$) ($K_n'$) and for the oxidised species $H_jL^{(j+2)+}$ ($Fe^{III}Fe^{III}$) ($K_n''$). The values obtained are shown in Table 7. Cyclic voltammetry experiments at pH 10 revealed a unique oxidation peak. By measuring $\Delta E_p$ and using the method reported by Richardson and Taube[28] a difference between the half-reaction potentials $E_5'$ and $E_5''$ of 80 mV was found. From this and the acid-dissociation constants previously obtained, the Pourbaix diagram for **2** has been calculated (see Fig. 6).

The Pourbaix diagram shows the shift of the p$K_a$ (vertical lines) to smaller values when the species $H_jL^{j+}$ ($Fe^{II}Fe^{II}$) are oxidised, indicating that the transformation of ferrocene to ferrocenium induces the compound to behave as a strong acid. Thus for example the dissociation constant for $HL^{3+}(Fe^{III}Fe^{III})$ is about one thousand times larger than that of $HL^+(Fe^{II}Fe^{II})$. The fact that the oxidation of the ferrocenyl group changes the acidity of the amino groups induces the molecule to give not only electrons but protons. Fig. 6 shows how in a wide pH range the oxidation of the reduced forms $H_jL^{j+}$ ($Fe^{II}Fe^{II}$) produces $H_{j-1}L^{j+1}$ ($Fe^{III}Fe^{III}$) or $H_{j-2}L^{j+}$ ($Fe^{III}Fe^{III}$) species in an overall reaction involving electron and proton transfer.

When a proton is co-ordinated to compound **2**, a positively charged nitrogen is created. The values of $E_4'$ and $E_4''$ compared with $E_5'$ and $E_5''$ give a good idea of how the presence of charged moieties changes the oxidation potential of the ferrocenyl group. Thus $E_4'$ is related to the oxidation potential of the ferrocenyl moiety which is further away from the positively charged nitrogen and the difference $E_4' - E_5' = 50$ mV represents the charge effect on that ferrocene group. On the other hand $E_4''$ is related to the oxidation potential of the nearest ferrocenyl group, which is expected to be more affected by the presence of a charged nitrogen. This is confirmed by the parameter $E_4'' - E_5'' = 160$ mV which is more than three times larger than $E_4' - E_5'$. When a second proton is co-ordinated a symmetric molecule containing two equivalent ferrocenyl groups is expected to be obtained. This seems to be in agreement with the value of $E_3' - E_4' = 120$ mV which is close

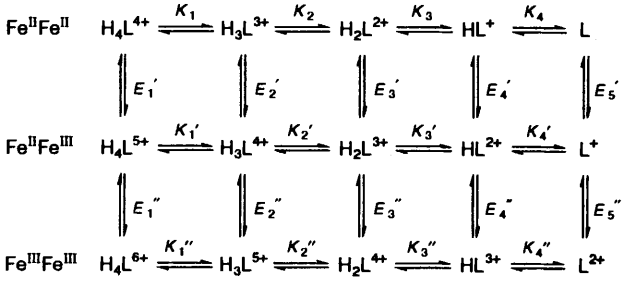


**Scheme 3** The charges shown are those for the whole species

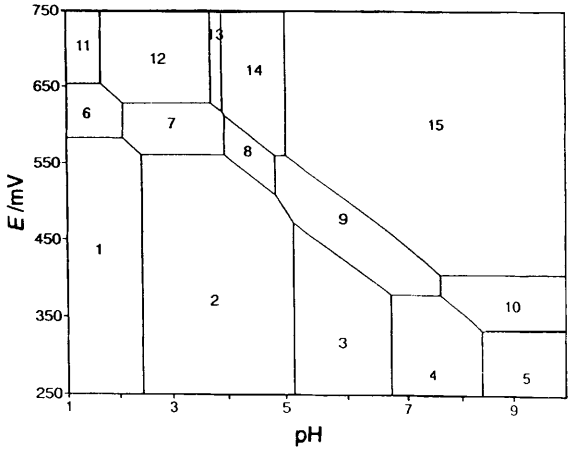


**Fig. 6** Diagram of oxidation potential *versus* pH for compound **2**. Species: 1, $H_4L^{4+}$ ($Fe^{II}Fe^{II}$); 2, $H_3L^{3+}$ ($Fe^{II}Fe^{II}$); 3, $H_2L^{2+}$ ($Fe^{II}Fe^{II}$); 4, $HL^+$ ($Fe^{II}Fe^{II}$); 5, L ($Fe^{II}Fe^{II}$); 6, $H_4L^{5+}$ ($Fe^{II}Fe^{III}$); 7, $H_3L^{4+}$ ($Fe^{II}Fe^{III}$); 8, $H_2L^{3+}$ ($Fe^{II}Fe^{III}$); 9, $HL^{2+}$ ($Fe^{II}Fe^{III}$); 10, $L^+$ ($Fe^{II}Fe^{III}$); 11, $H_4L^{6+}$ ($Fe^{III}Fe^{III}$); 12, $H_3L^{5+}$ ($Fe^{III}Fe^{III}$); 13, $H_2L^{4+}$ ($Fe^{III}Fe^{III}$); 14, $HL^{3+}$ ($Fe^{III}Fe^{III}$); 15, $L^{2+}$ ($Fe^{III}Fe^{III}$)

to the difference $E_4'' - E_5''$. In fact, a good agreement exists between the differences $E_n' - E_{n+1}'$ and $E_{n+1}'' - E_{n+2}''$. Further co-ordination of protons creates highly charged species and the effect that new positively charged nitrogens have on the ferrocenyl groups is not easily elucidated.

As we have determined above, the transition-metal ions copper(II), nickel(II) and zinc(II) form, with compound **2**, different species in solution as a function of the proton concentration. We have measured $E_{\frac{1}{2}}$ for the ferrocenyl groups as a function of pH when stoichiometric amounts of **2** and $M^{II}$ (M = Cu, Ni or Zn) are dissolved in thf–water (70:30 v/v). Data were taken under the same conditions at which the potentiometric measurements were carried out, with the $E_{\frac{1}{2}}$ values obtained from rotating-disc electrode experiments. Fig. 7 shows a plot of $E_{\frac{1}{2}}$ *versus* pH for the systems **2**–$H^+$ and **2**–$H^+$–$M^{II}$ (M = $Cu^{II}$, $Ni^{II}$ or $Zn^{II}$). Nickel(II) and zinc(II), for all the pH range studied, show similar $E_{\frac{1}{2}}$ values, in accord with the fact that they have similar distribution diagrams and quite close complex-formation constants. The plot of $E_{\frac{1}{2}}$ *versus* pH for $Cu^{II}$ is quite different to that of **2** and the nickel(II) or zinc(II) systems. At pH < 5 two waves were observed, one attributed to oxidation of the ferrocenyl groups and a cathodic wave corresponding to the presence of unco-ordinated copper(II), consistent with the distribution diagram (Fig. 3). From pH 5 to 10 $E_{\frac{1}{2}}$ is almost unchanged.

Recently it has been reported that using water-soluble polyaza and polyammonium ferrocene molecules the electrochemical recognition of transition-metal cations and phosphate anions in an aqueous environment can be achieved.[9] The recognition of metal ions was reported to be performed at pH > 10.5 at which the ligands were fully deprotonated. However to our knowledge a study of the shift of $E_{\frac{1}{2}}$ shifting in ligand–$H^+$–substrate systems as a function of pH has never been reported for redox-functionalised compounds.

**Table 7** Values of $pK_a$ and redox potential ($V$)* for $H_jL^{j+}(Fe^{II}Fe^{II})$, $H_jL^{(j+1)+}(Fe^{II}Fe^{III})$ and $H_jL^{(j+2)+}(Fe^{III}Fe^{III})$

| | | | | | | | |
|---|---|---|---|---|---|---|---|
| $pK_1$ | $pK_2$ | $pK_3$ | $pK_4$ | $pK_1'$ | $pK_2'$ | $pK_3'$ | $pK_4'$ |
| 2.45(3) | 5.15(1) | 6.71(1) | 8.40(1) | 2.08(8) | 3.96(6) | 4.85(5) | 7.62(3) |
| $pK_1''$ | $pK_2''$ | $pK_3''$ | $pK_4''$ | | | | |
| 1.66(18) | 3.72(17) | 3.92(18) | 5.03(12) | | | | |
| $E_1'$ | $E_2'$ | $E_3'$ | $E_4'$ | $E_5'$ | $E_1''$ | $E_2''$ | $E_3''$ |
| 0.58(1) | 0.56(1) | 0.51(1) | 0.38(1) | 0.33(1) | 0.65(1) | 0.63(1) | 0.61(1) |
| $E_4''$ | $E_5'$ | | | | | | |
| 0.56(1) | 0.41(1) | | | | | | |

* Values in parentheses are the standard deviations in the last significant digit.

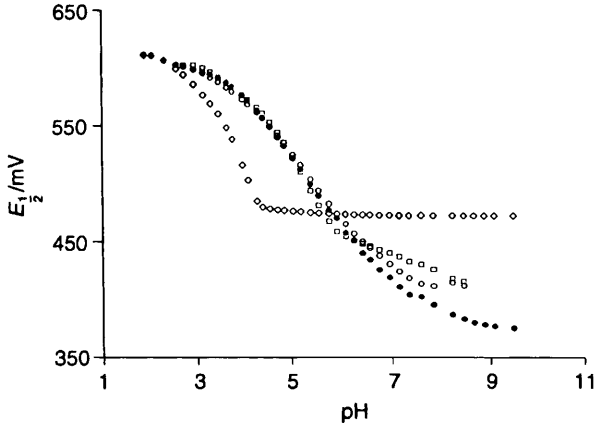


**Fig. 7** Plot of the half-wave potentials ($E_{\frac{1}{2}}$) *versus* pH for **2**–$H^+$ (●) and **2**–$H^+$–$M^{II}$ [M = Cu (◇), Ni (□) or Zn (○)]

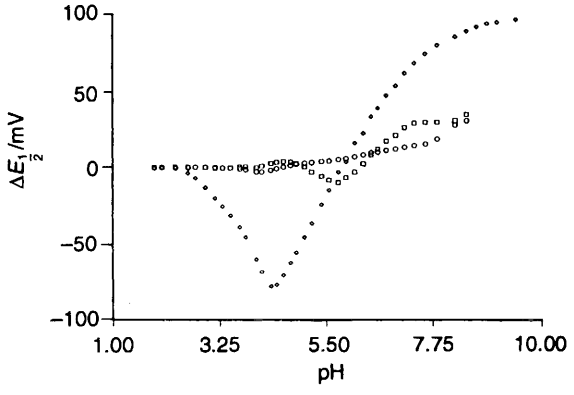


**Fig. 8** Plot of $\Delta E_{\frac{1}{2}}$ *versus* pH for copper(II) (◇), nickel(II) (□) and zinc(II) (○)

We have been able to fit the plot of $E_{\frac{1}{2}}$ for compound *versus* pH, and therefore the oxidation potential of the ferrocenyl groups can be calculated by use of an equation which is a function of the acidity constants of the reduced and oxidised species. In a similar manner we think that the $E_{\frac{1}{2}}$ value as a function of pH for the **2**–$H^+$–$M^{II}$ systems should also be related to the equilibrium constants of all the species existing in solution. We have made an attempt to fit the curves shown in Fig. 7 by use of a scheme similar to that proposed for **2**, but although the curve shapes could be simulated the constant values obtained are not completely satisfactory.

The fact that different metals cause a different shift in the oxidation potential of the ferrocenyl groups is a requirement for considering compound **2** to be a selective chemical sensor. From an electrochemical recognition viewpoint, more important than $E_{\frac{1}{2}}$ for the **2**–$H^+$–$M^{II}$ system is the relative value of $E_{\frac{1}{2}}$ compared with that of free **2**. Let us define the function $\Delta E_{\frac{1}{2}}$ as the difference between $E_{\frac{1}{2}}$ for **2**–$H^+$–$M^{II}$ and **2**–$H^+$ systems. A plot of $\Delta E_{\frac{1}{2}}$ *versus* pH for copper(II), nickel(II) and zinc(II) is shown in Fig. 8. At a fixed pH, $\Delta E_{\frac{1}{2}}$ represents the maximum shift that can be expected when **2** displays self-assembly processes with the corresponding transition-metal ion. A value $>0$ indicates that the addition of the metal shifts the redox potential to anodic potentials compared with that of the **2**, whereas when $\Delta E_{\frac{1}{2}} < 0$, $E_{\frac{1}{2}}$ is shifted to cathodic potentials. Copper(II) shows a maximum anodic displacement at pH 9.5 ($\Delta E_{\frac{1}{2}} = 97$ mV) and a maximum cathodic shift at pH 4.4 ($\Delta E_{\frac{1}{2}} = -78$ mV). The plot of $\Delta E_{\frac{1}{2}}$ *versus* pH for copper(II) shows a negative $\Delta E_{\frac{1}{2}}$ value over a wide pH range. That reveals that pH-responsive redox-active compounds can cause either positive or negative shifts by adequate tuning of the pH of the medium. To our knowledge, apart from a recently reported case when $\Delta E_{\frac{1}{2}}$ was negative, all the $\Delta E_{\frac{1}{2}}$ values known are positive.[10]

The existence of some pH regions where $\Delta E_{\frac{1}{2}} > 0$ and $<0$ implies that a pH must exist where $\Delta E_{\frac{1}{2}} = 0$. For copper(II), $\Delta E_{\frac{1}{2}} = 0$ at pH 5.9. Addition of copper(II) to a buffered solution of compound **2** at pH 5.9 does not produce any shift of the oxidation potential of the ferrocenyl groups and therefore the presence of copper(II) is *masked*. The presence of such *masked points* can also be observed for $Ni^{II}$ and $Zn^{II}$. This is of obvious importance in the design of new electrosupramolecular receptors because it would be possible to enhance the selectivity of a compound towards a substrate by adjusting the solution to a pH at which the electrochemical response to other substrates is *masked*. Unfortunately in our case, when $\Delta E_{\frac{1}{2}} = 0$ for copper the $\Delta E_{\frac{1}{2}}$ values for $Ni^{II}$ and $Zn^{II}$ are probably not large enough, and experiments designed electrochemically to recognise the presence of these ions at pH 5.9 in the presence of copper did not lead to a clear conclusion. Compound **2** can be considered as a selective electrochemical sensor for copper over a wide pH range. We have carried out some experiments to confirm the selectivity; for example at pH 4.4 an $\Delta E_{\frac{1}{2}}$ of about $-80$ mV is found when copper(II) is added to the solution even in the presence of nickel(II) or zinc(II) ions.

## Conclusion

The synthesis of receptors containing redox-active groups has been of great importance in the design of molecules for the electrochemical recognition of substrates. We have reported here how selectivity can be achieved by taking advantage of the fact that pH-responsive molecules can form several ligand–$H^+$ and ligand–$H^+$–substrate species as a function of pH. In these systems the oxidation potential seems to be a function of the formation constants for both reduced and oxidised species which exist in solution. The function $\Delta E_{\frac{1}{2}}$ represents the difference between the redox potential of **2**–$H^+$–$M^{II}$ and the **2**–$H^+$ systems. Taking into account that when $\Delta E_{\frac{1}{2}} \neq 0$ there is a recognition process, it can be concluded from Fig. 8 that a tuning of the electrochemical recognition ability of the ligand can be achieved by changing the pH in solution. This tuning can enhance the response towards a substrate or its presence can be *masked*.

## Acknowledgements

We thank the Dirección General de Investigación Científica y Técnica (proyecto PB91-0807-C02-02) and the SERC (to P. R. R.) for support. We are indebted to Professor A. Vacca and Dr. E. Gracía-España for help with the program SUPERQUAD.

## References

1 D. Astruc, *New. J. Chem.*, 1992, **16**, 305; P. D. Harvey and L. Gan, *Inorg. Chem.*, 1991, **30**, 3239.
2 *Energy Resources through Photochemistry and Catalysis*, ed. M. Grätzel, Academic Press, New York, 1983.
3 D. Astruc, J. R. Hamon, G. Althoff, E. Román, P. Batail, P. Michand, J. P. Mariot, F. Varret and D. Cozak, *J. Am. Chem. Soc.*, 1979, **101**, 5445; C. P. Andrieux, C. Blocman, J. M. Dumas-Bouchiat, F. M'Halla and J. M. Savéant, *J. Am. Chem. Soc.*, 1980, **102**, 3806; C. P. Andrieux, C. Blocman, J. M. Dumas-Bouchiat and J. M. Savéant, *J. Am. Chem. Soc.*, 1979, **101**, 3431; V. Guerchais, E. Román and D. Astruc, *Organometallics*, 1986, **5**, 2505; D. Astruc, M.-H. Desbois, M. Lacoste, F. Moulines, J. R. Hamon and F. Varret, *Polyhedron*, 1990, **9**, 2727.
4 J. A. Epstein and J. S. Miller, *Magnetic Molecular Materials*, eds. D. Gatteschi, O. Kahn, J. S. Miller and F. Palacio, NATO ASI Ser. No. 198, Kluwer, Dordrecht, 1990, pp. 151, 159.
5 T. Saji and I. Kinoshita, *J. Chem. Soc., Chem. Commun.*, 1986, 716; T. Saji, *Chem. Lett.*, 1986, 275; G. De Santis, M. Di Casa, L. Fabbrizzi, M. Licchelli and P. Pallavicini, *Adv. Mater.*, 1991, **3**, 611; G. De Santis, L. Fabbrizzi, M. Licchelli, A. Monichino and P. Pallavicini, *J. Chem. Soc., Dalton Trans.*, 1992, 2219.
6 P. D. Beer, *Chem. Soc. Rev.*, 1989, **18**, 409; R. E. Wolf and S. R. Cooper, *J. Am. Chem. Soc.*, 1984, **106**, 4646; P. D. Beer, C. J. Jones, J. A. McCleverty and S. S. Salam, *J. Incl. Phenom.*, 1987, **5**, 521; A. Kaifer, D. A. Gustowski, L. Echegoyen, V. J. Gratto, R. A. Schultz, T. P. Cleary, C. R. Morgan, D. M. Goli, A. M. Rios and G. W. Gokel, *J. Am. Chem. Soc.*, 1985, **107**, 1958; E. Fu, M. L. H. Green, V. J. Lowe and S. R. Marder, *J. Organomet. Chem.*, 1988, **341**, C39; L. Echegoyen, D. A. Gustowski, V. J. Gatto and G. W. Gokel, *J. Chem. Soc., Chem. Commun.*, 1986, 220; D. A. Gustowski, L. Echegoyen, D. M. Goli, A. Kaifer, R. A. Schultz and R. A. Gokel, *J. Am. Chem. Soc.*, 1984, **106**, 1633.
7 P. D. Beer, D. B. Crowe, M. I. Ogden, M. G. B. Drew and B. Main, *J. Chem. Soc., Dalton Trans.*, 1993, 2107; P. D. Beer, H. Sikanyika, C. Blackburn and J. F. Mc Aleer, *J. Chem. Soc., Chem. Commun.*, 1989, 1831; P. D. Beer, H. Sikanyika, A. M. Z. Slawin and D. J. Williams, *Polyhedron*, 1989, **8**, 879; M. P. Andrews, C. Blackburn, J. F. Mc Aleer and V. D. Patel, *J. Chem. Soc., Chem. Commun.*, 1987, 1122; P. D. Beer, 1990, 3295; P. D. Beer, H. Sikanyika, C. Blackburn, J. F. Mc Aleer and M. G. B. Drew, *J. Organomet. Chem.*, 1988, **356**, C19.
8 P. D. Beer, A. D. Keefe, H. Sikanyika, C. Blackburn and J. F. Mc Aleer, *J. Chem. Soc., Dalton Trans.*, 1990, 3289; M. C. Grossel, M. R. Goldspink, J. P. Knychala, A. K. Cheetham and J. A. Hriljac, *J. Organomet. Chem.*, 1988, **352**, C13; P. D. Beer, C. G. Crane, A. D. Keefe and A. R. Whyman, *J. Organomet. Chem.*, 1986, **314**, C9; N. D. Lowe and C. D. Garner, *J. Chem. Soc., Dalton Trans.*, 1993, 3333; C. Hall, J. H. R. Tucker, S. Y. F. Chu, A. W. Parkins and S. C. Nyborg, *J. Chem. Soc., Chem. Commun.*, 1993, 1505.
9 P. D. Beer, Z. Chen, M. G. B. Drew, J. Kingston, M. Ogden and P. Spencer, *J. Chem. Soc., Chem. Commun.*, 1993, 1046.
10 G. De Santis, L. Fabbrizzi, M. Licchelli, P. Pallavicini and A. Perotti, *J. Chem. Soc., Dalton Trans*, 1992, 3283.
11 J. C. Medina Goodnow, M. T. Rojas, J. L. Atwood, B. C. Lynn, A. E. Kaifer and G. W. Gokel, *J. Am. Chem. Soc.*, 1992, **114**, 10583; P. D. Beer and A. D. Keefe, *J. Organomet. Chem.*, 1989, **375**, C40; P. D. Beer, C. Hazlewood, D. Hesek, J. Hodacova and S. E. Stokes, *J. Chem. Soc., Dalton. Trans.*, 1993, 1327.
12 B. Dietrich, M. W. Hosseini, J. M. Lehn and R. B. Sessions, *J. Am. Chem. Soc*, 1981, **103**, 1282; M. W. Hosseini, J. M. Lehn, L. Maggiora, K. B. Mertes and M. P. Mertes, *J. Am. Chem. Soc.*, 1987, **109**, 537; M. W. Hosseini and M. W. Lehn, *Helv. Chim. Acta*, 1987, **70**, 1312; J. F. Marecek and C. J. Burrows, *Tetrahedron Lett.*, 1986, **27**, 5943; J. F. Marecek, C. P. A. Fischer and C. J. Burrows, *Tetrahedron Lett.*, 1988, **29**, 6231; E. Kumura, M. Kodama and T. Yatsunami, *J. Am. Chem. Soc.*, 1982, **104**, 3182; N. I. Manfrin, L. Moggi, V. Castelvetro, V. Balzani, M. W. Hosseini and J. M. Lehn, *J. Am. Chem. Soc.*, 1985, **107**, 6888; M. W. Hosseini, A. J. Blacker and J. M. Lehn, *J. Am. Chem. Soc.*, 1990, **112**, 3896.
13 A. Benito, J. Cano, R. Martínez-Máñez, J. Soto, J. Payá, F. Lloret, M. Julve, J. Faus and M. D. Marcos, *Inorg. Chem.*, 1993, **32**, 1197.
14 J. Cano, A. Benito, R. Martínez-Máñez, J. Soto, J. Payá, F. Lloret, M. Julve, M. D. Marcos and E. Sinn, *Inorg. Chim. Acta*, 1995, **231**, 45.
15 A. Benito, J. Cano, R. Martínez-Máñez, J. Payá, J. Soto, M. Julve, F. Lloret, M. D. Marcos and E. Sinn, *J. Chem. Soc., Dalton. Trans.*, 1993, 1999; A. Benito, J. Cano, R. Martínez-Máñez, J. Soto, M. J. L. Tendero, J. Payá and E. Sinn; *Inorg. Chim. Acta*, 1993, **210**, 233; E. C. Constable, A. J. Edwards, R. Martínez-Máñez, P. R. Raithby and A. M. W. Cargill Thompson, *J. Chem. Soc., Dalton Trans.*, 1994, 645; E. C. Constable, R. Martínez-Máñez and A. M. W. Cargill-Thompson, *J. Chem. Soc., Dalton Trans.*, 1994, 645; A. J. Edwards, M. D. Marcos, P. R. Raithby, R. Martínez-Máñez and M. J. L. Tendero, *Inorg. Chim. Acta*, 1994, **224**, 11.
16 G. G. A. Balavoine, G. Doisneau and T. Fillebeen-Khan, *J. Organomet. Chem.*, 1991, **412**, 381.
17 G. Gran, *Analyst (London)*, 1952, **77**, 661; F. J. Rossotti and H. J. Rossotti, *J. Chem. Educ.*, 1965, **42**, 375.
18 P. Gans, A. Sabatini and A. Vacca, *J. Chem. Soc., Dalton Trans.*, 1985, 1195.
19 SHELXTL PLUS, Version 4.0, Siemens Analytical X-Ray Instruments, Madison, WI, 1990.
20 G. M. Sheldrick, SHELXL 93, University of Göttingen, 1993.
21 M. J. L. Tendero, A. Benito, J. M. Lloris, R. Martínez-Máñez, J. Soto, J. Payá, A. J. Edwards and P. R. Raithby, *Inorg. Chim. Acta*, in the press.
22 H. Plenio, J. Yang, R. Diodone and J. Heinze, *Inorg. Chem.*, 1994, **33**, 4098.
23 M. Micheloni, A. Sabatini and P. Paoletti, *J. Chem. Soc., Perkin Trans.*, 1978, 828.
24 M. Kodama and E. Kimura, *J. Chem. Soc., Chem. Commun.*, 1975, 891.
25 A. Benito, R. Martínez-Máñez, J. Payá, J. Soto, M. J. L. Tendero and E. Sinn, *J. Organomet. Chem.*, 1995, **503**, 259.
26 W. M. Clark, in *Oxidation-Reduction Potentials of Organic Systems*, Williams & Wilkins Co., Baltimore, MD, 1960.
27 M. Haga, T. Ano, K. Kano and S. Yamabe, *Inorg. Chem.*, 1991, **30**, 3843; M. Haga, T. Ano, T. Ishizaki, K. Kano, K. Nozaki and T. Ohno, *J. Chem. Soc., Dalton Trans.*, 1994, 263.
28 D. E. Richardson and H. Taube, *Inorg. Chem.*, 1981, **20**, 1278.

*Received* 1*st June* 1995; *Paper* 5/03502C